

the maximum pile-up height and the indentation depth shows approximately a linear behaviour.

5. Behaviour of Pile-Up Effect with Material Properties

Simulations are done for the same specimen dimensions (same mesh characteristics) with the same indentation depth as 1000 nm to identify the pile-up effect on the specimen with varying material properties. In order to compare the material properties in simulations, the specimen's material properties are changed according to Table 1.

Table 1 - Models Simulated According to the Variation of Material Properties

Case No	Material properties		
	Strain hardening coefficient (n)	Yield strength (MPa)	Young's modulus (GPa)
1	Vary (0.1-0.48)	300	75
2	0.1	Vary (75-345)	75
3	0.1	300	Vary (50-240)

5.1 Behaviour of the Strain Hardening Component (n)

Strain hardening coefficient (n) is a measure of how much the metal can be strengthened by strain hardening. It needs to have some ductility to be strain hardened. In simple terms, n is the slope of the plastic portion of the true stress with the true strain curve when graphed on a logarithmic scale.

The selected load-displacement curves are obtained by using case 1, which is represented in Table 1. Figure 11 shows that, for a fixed indentation depth (1000 nm), load-displacement curves are varying with strain hardening coefficient.

The maximum load of a fixed indentation depth is linearly increasing with the strain hardening coefficient in the load-displacement curve shown in Figure 12. For the high hardness material, the strain hardening component is high. Therefore, the required force needs to penetrate for fixed indentation depth increases with strain hardening component. The unloading curve shows the same gradient without any change. That implies that Young's modulus is not varying in this scenario.

The pile-up profiles by varying the strain hardening coefficient are shown in Figure 13.

The correlation between maximum pile-up height with strain hardening coefficient is shown in Figure 14.

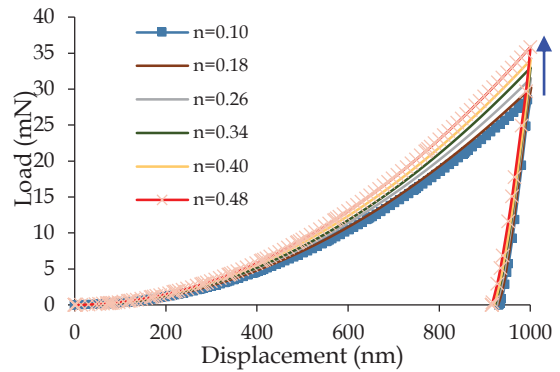


Figure 11 - Selected Load-Displacement Curves while Varying the Strain Hardening Coefficient

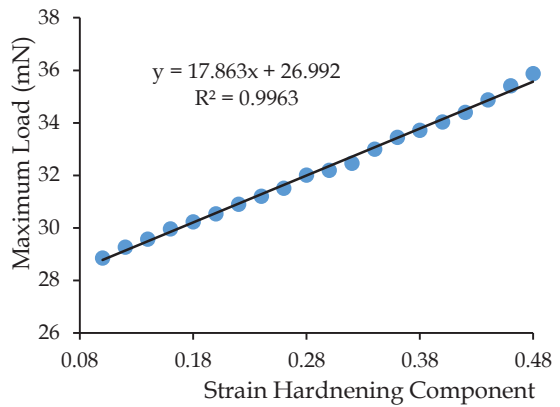


Figure 12 - The Maximum Indentation Load by Varying the Strain Hardening Coefficient

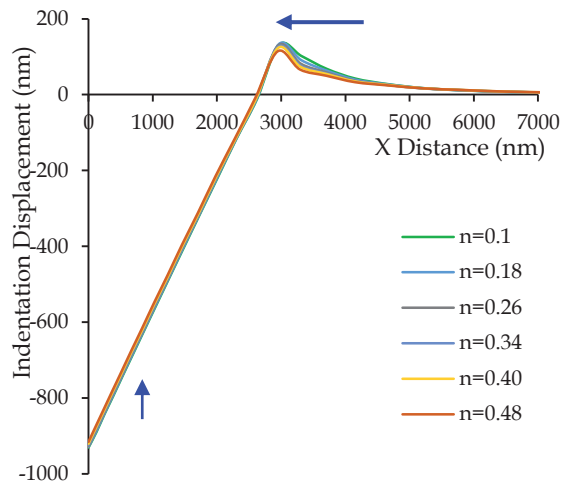


Figure 13 - Pile-Up Profiles by Varying the Strain Hardening Coefficient

As shown in Figure 14, with the increment of the strain hardening coefficient, the recovery depth of the indentation is increased.



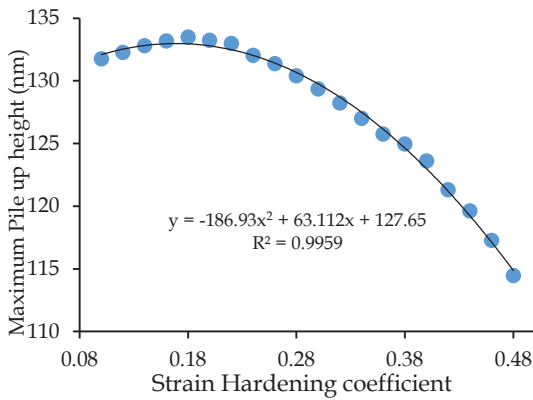


Figure 14 - The Variation of Maximum Pile-Up Height with the Strain Hardening Coefficient

5.2 Behaviour of the Yield Strength

The selected load-displacement curves, obtained by using case 2 (corresponding to Table 1), are presented in Figure 15. The unloading curves in Figure 15 show the same gradient without any changes in Young's modulus. As mentioned before, this implies that Young's modulus is not varying in this scenario.

Figure 16 shows that the maximum loads for a fixed indentation depth are linearly increasing with yield strength. With the increase of the yield strength, the material is getting hardened. It implies that the force needing for penetration is increasing with the yield strength for a fixed indentation depth.

The pile-up profiles by varying the yield strengths are shown in Figure 17. Correlation between maximum pile-up heights with yield strength is shown in Figure 18.

As shown in Figure 17, with the increase of the yield strength, the recovery depth of the indentation is increased. In the beginning, to control the pile-up volume, considering both strain hardening component and yield strength (Figures 13 and 17), the maximum pile-up height also increased. The shape of the outer surface of the pile-up profile declines gradually. However, from a certain point, pile-up volume starts to reduce. Similarly, the maximum pile-up height is also reduced. Because of this reason, the graphs in Figure 14 and Figure 18 are obtained as a parabolic path.

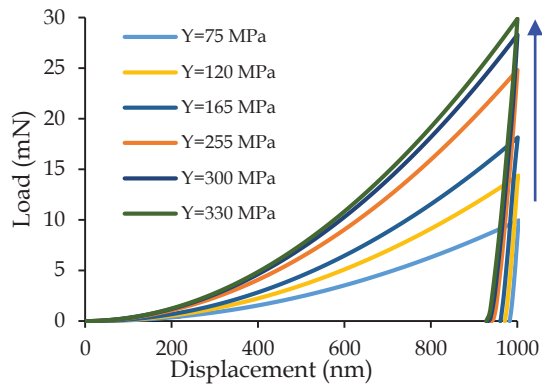


Figure 15 - Load-Displacement Curves while Varying the Yield Strength

5.3 Behaviour of the Young's Modulus

The selected load-displacement curves obtained using case 3 (corresponding to Table 1) are presented in Figure 19.

Figure 20 shows a variation of slopes in the unloading curves of the load-displacement curves. Considering Figure 19, it can be said that unloading slope depends on Young's modulus.

The maximum load of an indentation test increases with Young's modulus in the load-displacement curve, as shown in Figure 19. Because of the increment in Young's modulus, the material is getting harder, and it becomes difficult for penetrating to a certain indentation depth. The unloading curves show a variation of their slopes in the load-displacement curves.

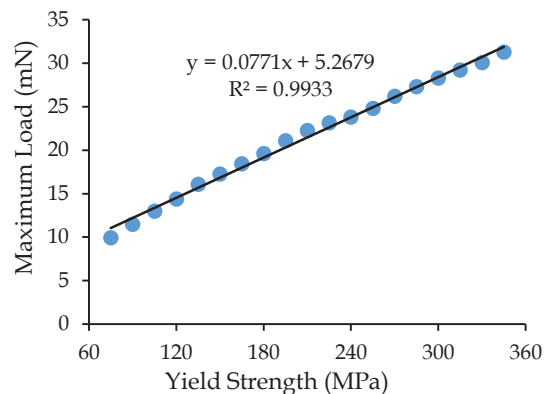


Figure 16 - The Maximum Indentation Load by Varying the Yield Strength

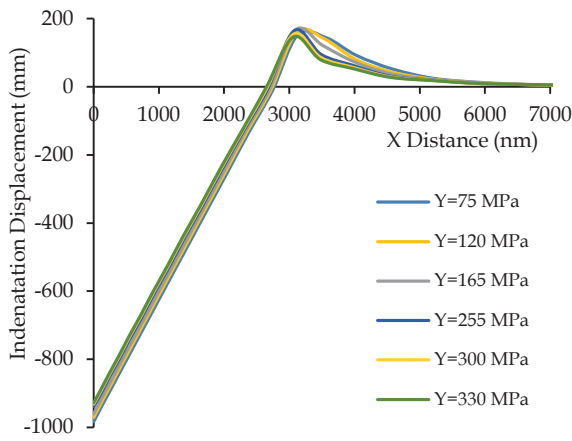


Figure 17 - Pile-Up Profiles by Varying Yield Strength

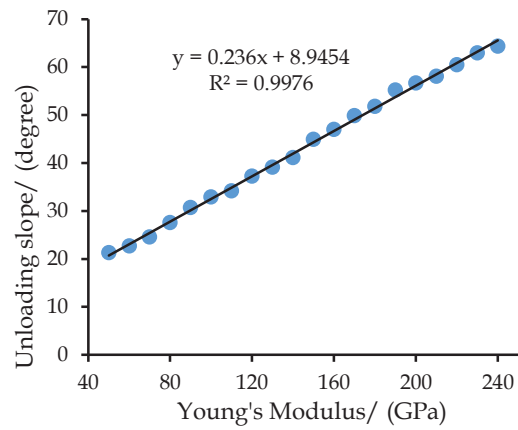


Figure 20 - The Slope of Unloading Curves with Varying Young's Modulus

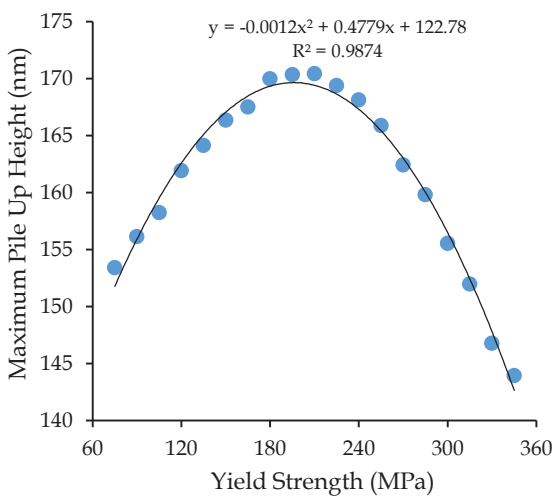


Figure 18 - The Variation of Maximum Pile-Up Height with Yield Strength

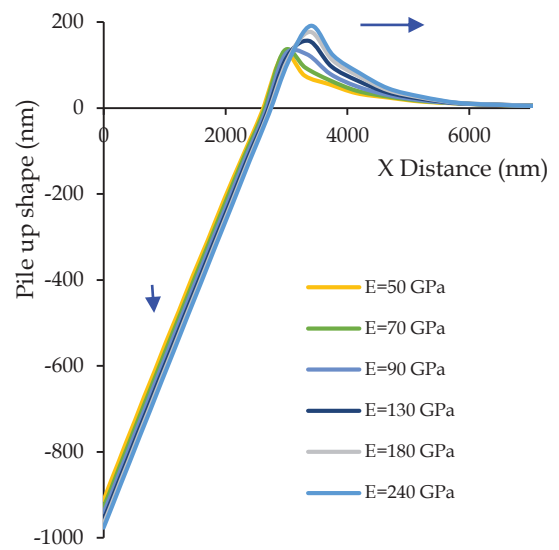


Figure 21 - Pile-Up Profiles by Varying Young's Modulus (E)

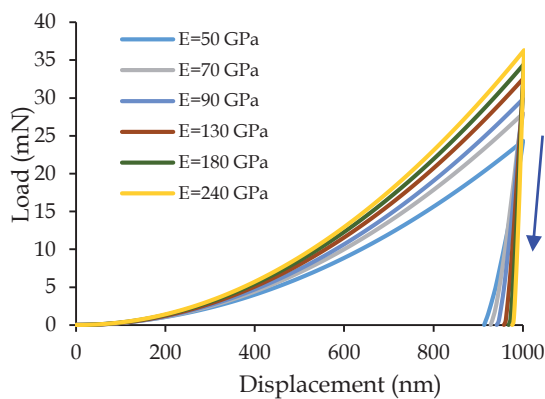


Figure 19 - Load-Displacement Curves while Varying Young's Modulus (E)

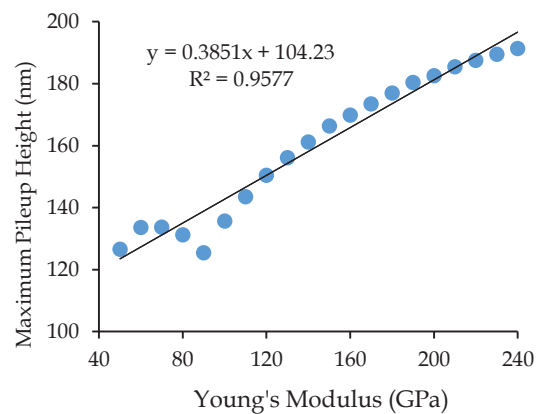


Figure 22 - The Variation of Maximum Pile-Up Height with Young's Modulus



The slope of unloading curves shows the linear relationship with Young's modulus, as shown in Figure 20. The pile-up profiles by varying Young's modulus are shown in Figure 21, where the maximum pile-up heights with Young's modulus are shown in Figure 22. Considering Figure 22, approximately maximum pile-up height is linearly varying with Young's modulus.

6. Conclusions

In this study, the pile-up effect on nanoindentation using numerical simulation is carried out. The main objectives of this study are to understand the behaviour of the pile-up effect on nanoindentation by using 2D and 3D numerical simulations and also to obtain correlations between the pile-up effect and material properties. Von Mises plasticity model is used for the specimen to get the real metal behaviour for the specimens. Two-dimensional FE models with cone indenter of half-angle 70.3° were used to replace the three-dimensional FE models with Berkovich indenter to simplify the simulation process. The conclusions made from the results are presented as follows.

- When indentation depth increases, pile-up height shows a linear behaviour. This relationship (Figure 10) can be used to find the approximate maximum pile-up value for this selected material.
- When varying the strain hardening coefficient and yield strength, approximately linear relationships are observed with the maximum indentation load (Figures 12 and 16) for a particular indentation depth. In addition to that, good relationships are obtained for maximum pile-up height, yield strength, and Young's modulus with strain hardening component (Figures 14, 18 and 22).
- Moreover, an approximately linear relationship is developed between Young's modulus and the unloading curve slope, as shown in Figure 20.
- All the relationships obtained from this study (Figures 12, 14, 16, 18, 20 and 22) can be used as an inverse analysis to extract the material parameters for other materials, which will help to develop further studies.

Acknowledgment

University Research Grant, URG/2018/23/E of the University of Peradeniya is highly appreciated.

References

1. ABAQUS/CAE User's Manual Version 6.14. (2016) Providence: ABAQUS, Inc.
2. Alaboodi, A. S., & Hussain, Z. (2017), "Finite Element Modeling of Nanoindentation Technique to Characterize Thin Film Coatings", *Engineering Sciences*, pp.1-9.
3. Belytschko, T., Ong, J. S. J., Liu, W. K., & Kennedy, J. M. (1984), "Hourglass Control in Linear and Nonlinear Problems", *Computer Methods in Applied Mechanics and Engineering*, Vol. 43, Issue 3, pp. 251-276.
4. Bhattacharyya, A. S. (2010), "Tribological and Surface Engineering Properties of SiCN Thin Films", *Proc. of the 3rd International Conference on Advances in Mechanical Engineering*.
5. Bolshakov, A., Oliver, W. C., & Pharr, G. M. (1996) "Influences of Stress on the Measurement of Mechanical Properties Using Nanoindentation", *Journal of Materials Research*, Vol.11(3), pp.760-768.
6. Bolshakov, A., & Pharr, G. M. (1998), "Influences of Pile-Up on the Measurement of Mechanical Properties by Load and Depth Sensing Indentation Techniques", *Journal of Materials Research*, Vol. 13, pp. 1049-1058.
7. Cabibbo, M., Ciccarelli, D., & Spigarelli, S. (2013), "Nano-Indentation Hardness Measurement in Piling Up SiO₂ Coating", *2nd European Conference on Nano Films*, Vol.40, pp.100-112.
8. Chen, X., Yan, J., & Karlsson, A. M. (2006), "On the Determination of Residual Stress and Mechanical Properties by Indentation", *Materials Science and Engineering: A*, Vol.416(1-2), pp.139-149.
9. Gale, J. D., & Achuthan, A. (2014), "The Effect of Work-Hardening and Pile-Up on Nanoindentation Measurements", *Journal of Materials Science*, Vol.49(14), pp.5066-5075.
10. Kralik, V., & Nemecek, J. (2014), "Comparing Nanoindentation Techniques for Local Mechanical Quantification of Aluminum Alloy", *Materials Science and Engineering*, Vol.618, pp.118-128.
11. Lichinchi, M., Lenardi, C., Haupt, J. & Vitali, R. (1998), "Simulation of Berkovich Nanoindentation Experiments on Thin Films Using Finite Element Method", *This Solid Films*, Vol.312, pp.240-248.
12. Moore, S. W., Manzari, M. T., & Shen, Y. L. (2010), "Nano-Indentation in Elastoplastic Materials: Insights from Numerical simulations", *International Journal of Smart and Nano Materials*, Vol.1:2, pp.95-114.

13. Oliver, W. C., & Pharr, G. M. (2004), "Measurement of Hardness and Elastic Modulus by Instrumented Indentation: Advances in Understanding and Refinements to Methodology", *Journal of Materials Research*, Vol. 19, pp. 3-20.
14. Sagadevan, S., & Murugasen, P. (2014), "Novel Analysis on the Influence of Tip Radius and Shape of the Nanoindenter on the Hardness of Materials", *3rd International Conference on Materials Processing and Characterisation, Procedia Materials Science*, Vol.6, pp.1871-1878.
15. Sivaram, S., Sutharsan, K., Jayasinghe, J. A. S. C., & Bandara, C. S. (2017), "Development of Indentation Testing Method for Evaluation of Mechanical Properties of Steel Reinforcement", *8th International Conference on Structural and Construction Management*, pp.85-93.
16. Sivaram, S., Jayasinghe, J. A. S. C., & Bandara, C. S. (2018), "Numerical Simulation of Indentation Test Method to Evaluate Residual Strain of Metals", *Advances in Civil and Environmental Engineering Practices for Sustainable Development*, pp.302-308.
17. Sivaram, S., Jayasinghe, J. A. S. C., & Bandara, C. S. (2018), "Prediction of Residual Strain of Steel Using Brinell Hardness Number: Development and Application to Old Bridge Structures in SriLanka", *Society of Structural Engineers Sri Lanka*, pp.79-85.
18. Sullivan, M. (2015), "Measuring, Evaluating and Describing Pile-Up and Sink-In During Nanoindentation of Thin Films on Substrates".
19. Von Mises, R. (1913), "Mechanics of Solid Bodies in a Plastically Dformable State", *Mathematical-Physics*, Vol. 1, pp. 582-592.
20. Zhao, M., Chen, X., Yan, J., & Karlsson, A. M. (2006), "Determination of Uniaxial Residual Stress and Mechanical Properties by Instrumented Indentation", *Acta Materialia*, Vol. 54(10).

